CHINESE JOURNAL OF PHYSICS VOL. 50, NO. 1 February 2012

The Optical and Structural Properties of ZnO Thin Films Deposited by the Spray Pyrolysis Technique

S. Aydogu,* O. Sendil, and M. B. Coban

Dumlupinar University, Faculty of Art and Science, Department of Physics, Kutahya, Turkey

(Received March 30, 2011)

ZnO films were deposited by the chemical spray pyrolysis technique at the substrate temperature of 350 ± 5 °C. Totally 200 cc of ZnO solution was sprayed at 5 ml/min controlled by a flowmeter. Nitrogen gas was used as the carrier gas. XRD measurement revealed the improvement of crystalline quality and grain size of the film as the polycrystalline structure (the hexagonal wurtzite structure) and 15.092 nm, respectively. An absorbance spectrum was taken to examine the optical properties, energy band gap, lattice parameters, refractive index, extinction coefficient, and dielectric function. The band gap and the energy levels of the defects of the ZnO film were calculated by the optical method as 3.20 eV and 2.40 eV. The dielectric function of the film was determined by the transmittance spectrum.

PACS numbers: 77.55.hf, 78.20.Ci, 81.15.Rs

I. INTRODUCTION

In recent years zinc oxide (ZnO) used as a transparent conducting oxide has been one of the most remarkable materials. ZnO has a large band gap, high conductivity, ease in doping, chemical stability in hydrogen plasma, thermal stability when doped with group III elements, relatively large exciton binding energy ($\sim$ 60 meV), abundance in nature, and no toxicity [1–7]. Zinc oxide (II–VI group) is an n-type semiconductor with the structure of hexagonal wurtzite and a direct allowed gap with a band gap of 3.3 eV at room temperature [8]. With these properties, there are very large fields of application in industrial and scientific research, particularly for both micro-electronic and optoelectronic devices. Zinc oxide is applied in transparent conductors, solar cell windows, heat mirrors, gas sensors, and surface acoustic wave (SAW) devices [9–14].

There are several techniques for producing ZnO semiconductor thin films. These techniques are molecular beam epitaxy (MBE) [15], chemical vapour deposition (CVD) [16], vacuum evaporation (VE) [17], sputtering [18], pulsed laser deposition (PLD) [19], electrochemical deposition [20], and spray pyrolysis methods (SP) [21, 22]. Among these techniques, the spray pyrolysis technique is particularly attractive due to the ease of composition control, large area coating, and low equipment cost. Compared with other techniques, the spray pyrolysis technique has advantages, such as a high purity of powders, excellent control of chemical uniformity, and stoichiometry in multi-component systems. Furthermore,

*Electronic address: saydogu@dumlupinar.edu.tr

 © 2012 THE PHYSICAL SOCIETY OF THE REPUBLIC OF CHINA

the optical, structural, and electrical properties of thin films can be easily controlled by the quantity of sprayed solution in this technique. In general, the films produced with this technique are polycrystalline, stable, uniform, adherent, and hard. Spray pyrolysis has been developed as a powerful tool for synthesizing various kinds of power materials such as metals, metal oxides, superconducting materials, and nanophase materials.

There have been extensive studies on the fabrication structure, electrical, and optical properties of ZnO. However, there are few reports on the dielectric function, optical constants, and absorption coefficients of ZnO films in the photon energy range of 1–5 eV. In this paper, we report on the optical and structural properties of ZnO film produced by the spray pyrolysis technique for application as an antireflective in solar cells, and present various optoelectronic parameters, such as the energy band gap, lattice parameters, refractive index, extinction coefficient, and dielectric constants.

II. EXPERIMENTAL

The zinc oxide (ZnO) film was deposited on glass substrates with the particular substrate temperature by the spray pyrolysis technique. The ZnO film was prepared as a solution of high purity zinc acetate dehydrate ($Zn(CH_3COO)_2.2H_2O$) at 0.3 M prepared in distilled water (1000 ml). The microscope glass substrates (1x1 cm^2) were cleaned before deposition first with detergent solution, then with alcohol, and last with deionised water. The cleaned substrates were disposed on the area of an electrical heater of 49 cm^2 and were heated by this electrical heater. The substrate temperature was controlled using a chrome-alum thermocouple. During the spray process, the substrates were kept at a constant temperature of $350 \pm 5\,°C$. The distance between the nozzle and heater was taken as about 28 cm. Totally 200 cc of ZnO solution was sprayed during 40 min at 5 ml/min (controlled by a flowmeter). The nitrogen carrier gas pressure was kept at the constant value of 0.2 kg/cm^2. At the end of the spraying process, the carrier gas and heater were slowly closed, and the glass substrates were given up to cooling for 4–5 hours in an air atmosphere. For the growth of good quality films, the experimental conditions, such as the distance between the nozzle and heater, the solution flow rate, the substrate temperature, and the carrier gas pressure were optimized [8, 22, 24, 25].

The deposited film was subjected to X-ray diffraction (XRD) analyses for structural identification, using a Rigaku Rint 2200 X-ray diffractometer with Cu K_α radiation ($\lambda =$ 1.54056 Å) at 40 kV and 30 mA. The optical measurement was made using the Shimadzu UVmini 1240 spectrophotometer, and all measurements were carried out at room temperature. The film thickness was obtained as 357 nm by the weight difference method using an electronic high precision balance.

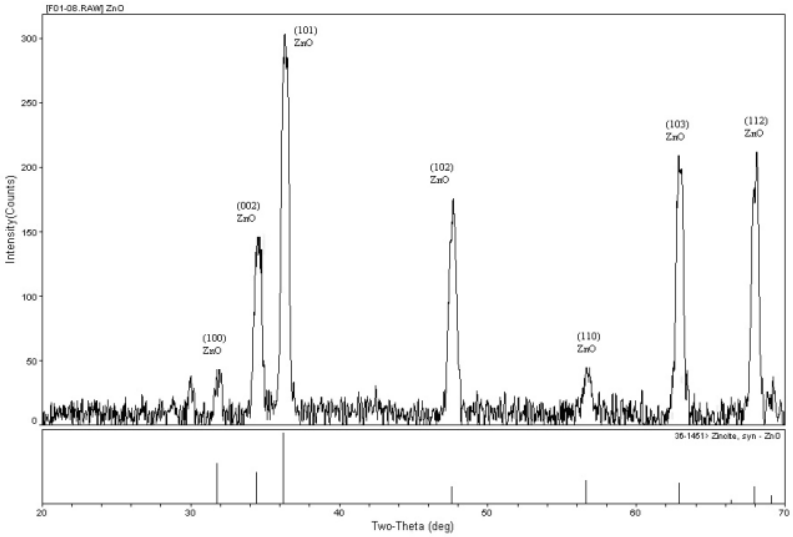

FIG. 1: XRD pattern of ZnO thin film deposited on glass substrate.

III. RESULTS AND DISCUSSION

The structural and optical properties of ZnO film deposited on glass substrate by the chemical spray pyrolysis technique were investigated. The structural properties of the ZnO film was investigated by the X-ray diffraction pattern ($20° < 2\theta < 70°$). Figure 1 shows the XRD pattern of the ZnO thin film. It shows that the peaks in this pattern have different intensities and full width at half maximum (FWHM). All the peaks of the XRD pattern are indexed to ZnO film crystallized in the polycrystalline structure, possessing the hexagonal wurtzite structure (PDF #36-1451).

The diffraction peaks in Fig. 1 are clearly identifiable. The most prominent peak observed in the ZnO film corresponds to the (1 0 1) plane. The peak of the (1 0 1) plane is the strongest XRD line for the standard zinc oxide powdered sample. Therefore their positions are very close to that of the standard diffraction patterns for ZnO powders [14]. Other planes corresponding to (1 0 0), (0 0 2), (1 0 2), (1 1 0), (1 0 3), and (1 1 2) have lower relative intensities. The intensities of the peaks of the ZnO film are different from the intensities of the peaks of the standard. In spray pyrolysis decomposition, the impinging atoms on the substrate undergo an endothermic reaction with the substrate surface, resulting in a heterogeneous type of growth. The arrangements of atoms in further layers get gradually modified by preceding layers. As a result, the growth takes place in a more definite way, resulting in a particular type of preferred growth, and differences in the intensities of peaks when the substrate temperature or other production conditions are changed are observed [2, 6]. In Table I the diffraction angles (2θ) in the diffraction pattern, the spacing (d), and the phases defined with the (hkl) planes of the ZnO thin film are given.

The lattice constants of ZnO film can be calculated from the most prominent peaks.

TABLE I: The values of X-ray diffraction peaks of ZnO thin film.

	Calculated			**PDF#36 - 1451**		
Film	**2θ**	**(hkl)**	**d(Å)**	**2θ**	**(hkl)**	**d(Å)**
ZnO	31.940	(100)	2.7997	31.768	(100)	2.8143
ZnO	34.500	(002)	2.5976	34.421	(002)	2.6033
ZnO	36.340	(101)	2.4701	36.252	(101)	2.4759
ZnO	47.680	(102)	1.9058	47.538	(102)	1.9111
ZnO	56.650	(110)	1.6235	56.602	(110)	1.6247
ZnO	62.870	(103)	1.4770	62.862	(103)	1.4771
ZnO	68.130	(112)	1.3752	67.961	(112)	1.3782

The lattice constants for the hexagonal structure are taken as a=b≠c. The a, b, and c lattice constants of ZnO with the hexagonal wurtzite structure were 0.32328 nm (a = b), 0.51952 nm, respectively. It is clear that the calculated lattice constants are found to be in good agreement with the PDF standards for ZnO powder [26, 27] (Table II).

TABLE II: The lattice constants of ZnO film.

	Calculated			**PDF#36 - 1451**		
Material	**a(Å)**	**b(Å)**	**c(Å)**	**a(Å)**	**b(Å)**	**c(Å)**
ZnO	3.2328	3.2328	5.1952	3.24982	3.24982	5.20661

The grain size (D) and dislocation density (δ) are calculated for the preferential orientation to obtain information about its crystalline level. The broadening of the full width at half maximum is inversely proportional to the grain size according to Scherrer's formula. The grain size D can be calculated with the following equation [26]:

$$D = \frac{0.9\lambda}{\beta \cos\theta} \tag{1}$$

with the angle position of the peak (θ) and the FWHM (β). In Equation (1), λ is the wavelength of the incident X-ray. The value of the crystallite size is estimated from Scherrer's formula (Eq. 1) as 15.092 nm. Our calculated value is nearly the same value as in the literature [28–31].

The dislocation density (δ) is described as the length of dislocation lines per unit volume of the crystal [32]. The dislocation density of the crystal gives information about the crystal structure. The dislocation density for preferential orientation can be calculated using the formula given below [33],

$$\delta = \frac{1}{D^2}. \tag{2}$$

The dislocation density is obtained from Equation (2) as 4.3905 $\times 10^{-3}$ (nm)$^{-2}$. The smaller the dislocation density is the better the crystallization of the film.

The absorption and the transmission spectra of ZnO film are shown in Figure 2 (a) and (b), respectively. It can be seen that the absorbance of the ZnO film is high at short wavelengths ($\lambda < 380$ nm) and low at long wavelengths ($\lambda > 380$ nm). The intrinsic absorption in a semiconductor occurs for wavelengths in the vicinity of the energy gap. The absorption coefficient α is calculated using Lambert's law [6]:

$$\alpha = \frac{\ln(1/T)}{t}, \tag{3}$$

where T is the transmittance and t is the film thickness. So, the transmittance of ZnO film is the inverse of its absorbance, namely the transmittance is low at short wavelengths and high at long wavelengths. This means that the film behaved as an opaque material due to its high absorbing properties at short wavelengths and as a transparent material at long wavelengths [24]. In Figure 2(b) it is shown that the transmission of ZnO film is high over large wavelengths. ZnO film exhibits a high average transmittance ($\sim 73.9\%$) in the visible region. This suggests that the produced film indicates a good optical quality due to low scatter or absorption losses.

The energies of photons of the incident light are sufficient for the excitation of electrons from the valance band to the conduction band, if they are equal to or bigger than the band gap of ZnO film. But, the oxygen vacancies and interstitial Zn are responsible for the conductivity of ZnO film [34]. Since these impurities can be ionized by the low energies of the incident light, ZnO thin film has small absorbance and high transmittance values at large wavelengths. The wavelength range in which this transition occurs is in the range of about 380–400 nm. This range refers to the fundamental absorption region. The dependence of the absorption coefficient on the photon energy in the high absorption region is worked out to obtain detailed information about the energy band gaps. Assuming that the transition becomes constant at the absorption edge, the absorption coefficient can be ascribed as a function of the incident photon energy as

$$\alpha h\nu = B(h\nu - E_g)^n, \tag{4}$$

where α is the absorption coefficient, $h\nu$ is the photon energy, E_g is the optical band gap and B is the slope of the Tauch edge, called the band tailing parameter. In the above equation $n = 1/2$ for a direct allowed transition, $n = 3/2$ for a direct forbidden transition, $n = 2$ for an indirect allowed transition, and $n = 3$ for an indirect forbidden transition [35]. Whether the film has direct or indirect band gaps is determined from the linearity of the plots of $(\alpha h\nu)^2$ versus $(h\nu)$ and $(\alpha h\nu)^{1/2}$ versus $(h\nu)$, respectively. From Fig. 3, the square of the absorption coefficient multiplied by the photon energy $(\alpha h\upsilon)^2$ is plotted as a function of the photon energy $(h\nu)$, and the band gap is obtained by extrapolating the linear portion of curve to the zero of $(\alpha h\nu)^2$. Namely, $n = 1/2$. Fig. 3 shows the typical $(\alpha h\nu)^2$ versus $(h\nu)$ graph of zinc oxide film. The band gap of the ZnO film is obtained as a direct band gap by the optical method, which was described above.

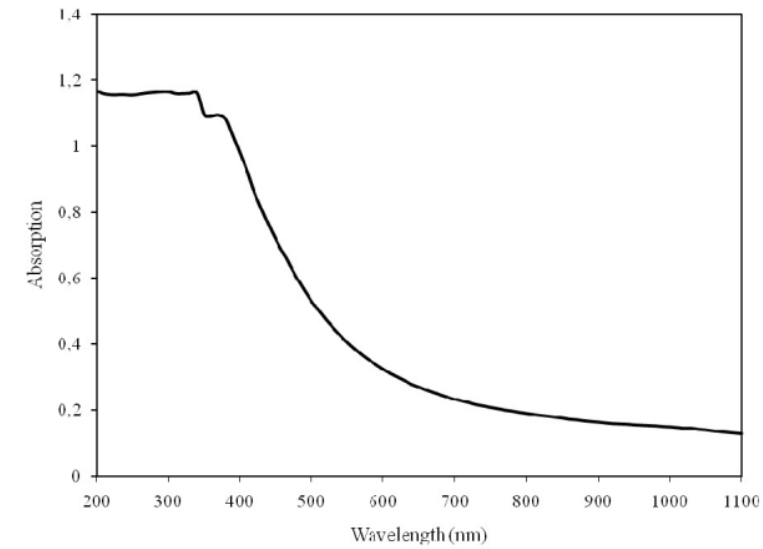

(a)

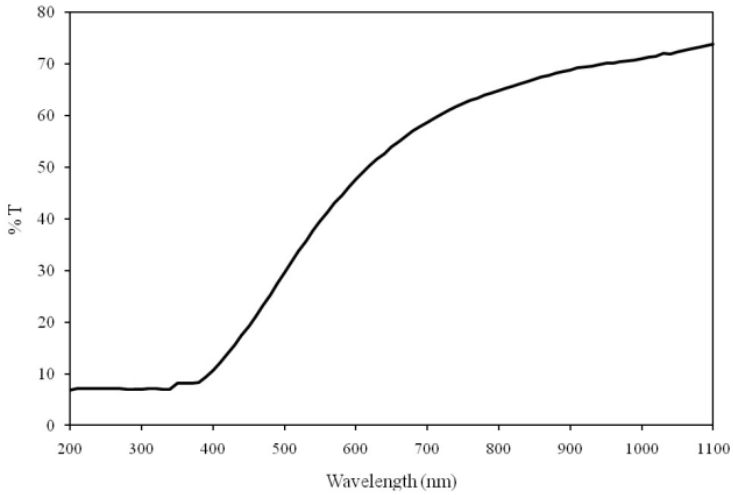

(b)

FIG. 2: Absorbance **(a)** and transmittance **(b)** spectra of ZnO film.

Figure 3 shows that ZnO film has two energy values. The first energy value (E_{g_1}) refers to the band to band transitions. This means that this energy value is the forbidden energy gap value of ZnO film. It was found as $E_{g_1} = 3.20$ eV from the $(\alpha h\nu)^2$ - $(h\nu)$ graph. The second energy E_{g2} is the transition energy to the energy levels of impurities and defects which are distributed inside the forbidden energy gap. Vanheusden *et al.* [36] suggested that ZnO powders show a strong visible emission band (525 nm = 2.35 eV) in the PL and one obvious mechanism responsible for the green emission might be originating from the commonly assumed recombination of photoexcited holes with electrons occupying the

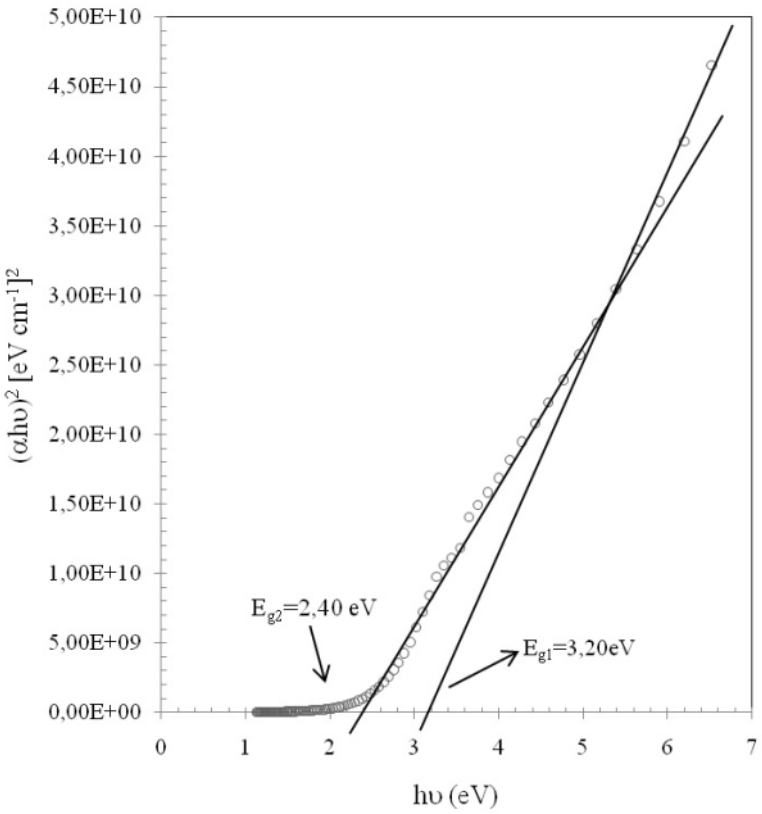

FIG. 3: $(\alpha h\nu)^2$ - $(h\nu)$ graph for ZnO film.

singly ionized oxygen vacancies. In Ref. [27], the green emission of ZnO thin films grown on polycrystalline α-alumina substrates by the ultrasonic spray pyrolysis (USP) technique was obtained as 2.48 eV. In this work, the second energy value (E_{g2}) is obtained as $E_{g2} = 2.40$ eV from Fig. 3. Our obtained value is quite compatible with the literature values [27, 36].

The reflectance R of a material with transmittance (T) and absorbance (A) is given by the relation below:

$$R = 1 - (Te^{A})^2. \tag{5}$$

The reflection spectrum of ZnO thin film is shown in Fig. 4. The reflection values are low for λ >380 nm, because this film has high transmittance and low absorbance values.

The other important parameter for thin films is the refractive index (n) of the film. The refractive index is closely related to the electronic polarizability of ions and the local field inside materials. Because of this it is one of the principle parameters for optical materials. The appraisal of the refractive index of optical materials is notably important for the applications in integrated optic devices (switches, filters, modulators, etc.) [35]. The refractive index (n) and the extinction coefficient (k) of film are calculated from the

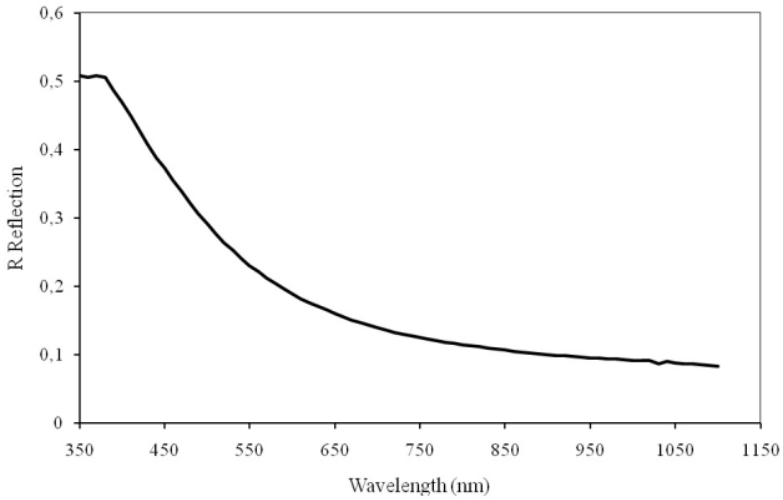

FIG. 4: Reflection spectrum of ZnO film.

equations below:

$$n = (1 + R)/(1 - R) + (4R/(1 - R)^2 - k^2)^{1/2}, \tag{6}$$

$$k = \frac{\alpha\lambda}{4\pi}, \tag{7}$$

where α is the absorption coefficient. As shown in Fig. 5, for ZnO film the refractive index first increases with the wavelength and then decreases after reaching a maximum value in the wavelength range 380 nm to 420 nm.

The dielectric constant of the material is a quantity related to the refractive index and a measure of the insulation [6]. The dielectric constant of ZnO film is expressed with the following relation:

$$\varepsilon(\omega) = \varepsilon_r(\omega) + \varepsilon_i(\omega), \tag{8}$$

where ε_r and ε_i are the real and imaginary parts of the dielectric constant. The real and imaginary dielectric constants can be calculated with the equations below:

$$\varepsilon_r = n^2 - k^2, \tag{9}$$

$$\varepsilon_i = nk, \tag{10}$$

where n and k are the refractive index and the extinction coefficient of film, respectively. Fig. 6 shows the variation of the real and imaginary parts of the dielectric constant with

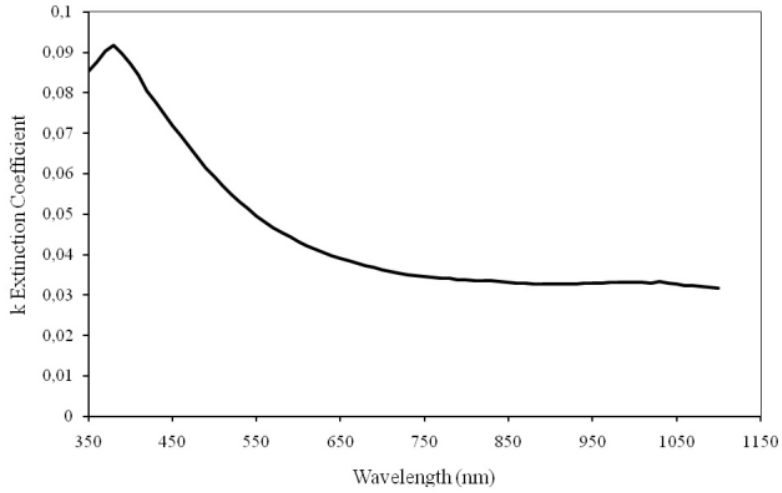

(a)

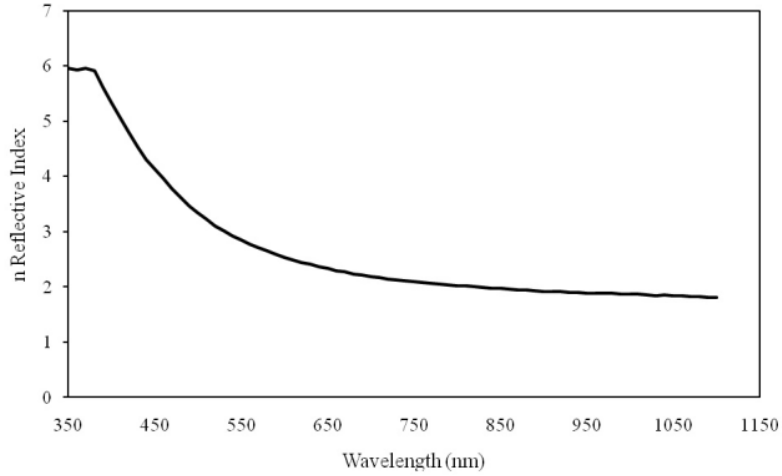

(b)

FIG. 5: Variation of the extinction coefficient **(a)** and the refractive index **(b)** of the ZnO film.

the incident wavelength. It is shown in Fig. 6 that the variations of the real and imaginary dielectric constants increase with decreasing wavelength of light.

As shown in Fig. 6(a), the real dielectric constant ε_r increase as the wavelength of light increases, later it reaches a maximum and finally decreases with increasing wavelength. This peak can correspond nearly to the optical band gap of the ZnO film, which is connected with the interband transition between the valence and conduction bands [37]. The imaginary dielectric constant graph is similar to the real dielectric constant graph. The significant imaginary dielectric constant ε_i also shows a significant peak in Fig. 6(b). The energy position of the absorption peak from an electronic transition corresponds to the peak transition energy obtained by the Tauch-Lorentz model [37, 38].

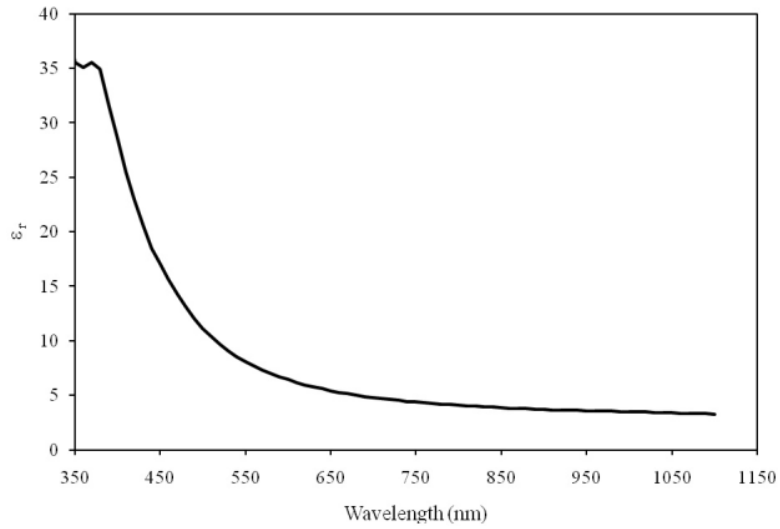

(a)

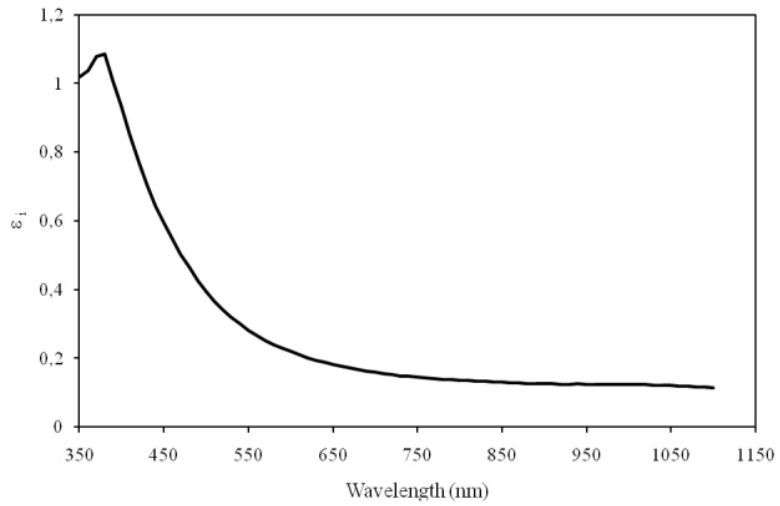

(b)

FIG. 6: The real **(a)** and the imaginary **(b)** parts of the dielectric constants of the ZnO thin film.

IV. CONCLUSIONS

The zinc oxide film was produced on the glass substrate temperature of $350 \pm 5\,^{\circ}\mathrm{C}$ by chemical spray pyrolysis technique. The optical, structural properties, and the dielectric function of the ZnO film are researched. It is seen that the ZnO film has a polycrystalline structure with a hexagonal wurtzite structure. The a (a=b) and c lattice constants of ZnO are calculated as 0.32328 nm and 0.51952 nm, respectively. The dislocation density of ZnO film with the crystallite size of 15.092 nm is obtained as 4.3905×10^{-3} $(\mathrm{nm})^{-2}$. The

transmittance of the produced ZnO has a low value at short wavelengths ($\lambda < 380$ nm) and a high value at long wavelengths ($\lambda > 380$ nm). From these optical investigations, it was found that ZnO behaved as an opaque material. It was shown that the fundamental absorption region of ZnO film is about 380–400 nm. ZnO has a direct band gap which is suitable for photovoltaic solar cells. The energy gap was calculated as 3.20 eV from the $(\alpha h\nu)^2$ - $(h\nu)$ graph. For ZnO thin films, it was shown that the energy value at about 2.40 eV (518 nm), may originate from the commonly assumed recombination of photoexcited holes with electrons occupying the singly ionized oxygen vacancies. The reflection value of ZnO film is low for $\lambda > 380$ nm, because this film has high transmittance and low absorbance values. The refractive index for ZnO film has its maximum value in the wavelength range of 380–420 nm. The real and imaginary parts of the dielectric function of ZnO film at a short wavelength range have a maximum value. The maximum value of the dielectric constant real part is 370 nm (3.35 eV) and the maximum value of the dielectric constant imaginary part is 340 nm (3.36 eV).

In other spray pyrolysis studies, ZnO thin films were growth on both glass [1, 6, 8–10, 12–14, 22] and Si (100) or Al_2O_3 [2, 27, 38, 39] substrates at high temperature (450–500 °C). Furthermore, the experimental parameters, such as molarities and flow rates of precursor solutions, carrier gases, and the distances between nozzle and heater, have varied from study to study. Comparing our work with other works, it can be seen that quality thin films could be produced with polycrystalline structure growth at lower substrate temperature, and the values of the energy band gaps of ZnO thin films are obtained as very close to the values in the literature [8, 13, 14, 39].

Acknowledgements

This research was supported by the Research Fund of Dumlupinar University, Kutahya, Turkey (Project No.: 2008-3).

References

[1] Y. Belghazi *et al.*, Microelectronj. **40**, 265–267 (2009).
[2] D. R. Acosta, L. Castaneda, A. Lopez-Suarez, and A. Guillen-Santiago, Phys. B **404**, 1427–1431 (2009).
[3] C. K. Ghosh, S. Das, and K. K. Chattopadhyay, Phys. B **399**, 38–46 (2007).
[4] C.-H. Choi and S-H. Kim, J. Cryst. Growth **283**, 170–179 (2005).
[5] J. Garnier, A. Bouteville, J. Hamilton, M. E. Pemble, and I. M. Povey, Thin Solid Films **518** (4), 1129–1135 (2009).
[6] B. Joseph, P. K. Manoj, and V. K. Vaidyan, Ceram. Int. **32**, 487–493 (2006).
[7] Z. W. Li, W. Gao, and R. J. Reeves, Surf. Coating. Tech. **198**, 319–323 (2005).
[8] J. Wienke and A. S. Booij, Thin Solid Films **516** (14), 4508–4512 (2008).
[9] J. Rodriguez-Baez, A. Maldonado, G. Torres-Delgado, R. Castanedo-Perez, M. de la L. Olvera, Mater. Lett. **60**, 1594–1598 (2006).

[10] H. Gomeza, A. Maldonado, M. de la L. Olvera, and D. R. Acosta, Sol. Energ. Mater. Sol. Cell **87**, 107–116 (2005).
[11] Z. Liu, Lei E, J. Ya, and Y. Xin, Appl. Surf. Sci. **255**, 6415–6420 (2009).
[12] M. A. Lucio-Lopez, M. A. Luna-Arias, A. Maldonado, M. de la L. Olvera, and D. R. Acosta, Sol. Energ. Mater. Sol. Cell **90**, 733–741 (2006).
[13] R. Martins *et al.*, Mater. Sci. Eng. B **118**, 135–140 (2005).
[14] P. P. Sahay and R. K. Nath, Sensor. Actuator. B **133**, 222–227 (2008).
[15] Z. Jin *et al.*, J. Cryst. Growth **214/215**, 55–58 (2000).
[16] P. Amezaga-Madrid, W. Antunez-Flores, R. J. Saenz-Hernandez, R. Martinez-Sanchez, and M. Miki-Yoshida, J. Alloy. Comp. **483**, 410–413 (2009).
[17] K. Iwata *et al.*, Thin Solid Films **451–452**, 219–223 (2004).
[18] Y. J. Park, H. N. Kim, and H. H. Shin, Appl. Surf. Sci. **255**, 7532–7536 (2009).
[19] A. Mitra and R. K. Thareja, J. Appl. Phys. **89**(4), 2025–2028 (2001).
[20] C. Y. Tsay, K-S. Fan, S-H. Chen, and C-H. Tsai, J. Alloy. Comp. **495**, 126–130 (2010).
[21] N. L. Tarwal and P. S. Patil, Appl. Surf. Sci. **256**, 7451–7456 (2010).
[22] N. Kavasoglu and A. S. Kavasoglu, Phys. B **403**, 3159–3163 (2008).
[23] M. Caglar, S. Ilcan, Y. Caglar, and F. Yakuphanoglu, J. Mater. Sci: Mater. Electron. **19**, 704–708 (2008).
[24] B. Ergin, E. Ketenci, and F. Atay, Int. J. Hydrogen. Energ. **34**, 5249–5254 (2009).
[25] M. Bizarro, Appl. Catal. B: Environ. **97**, 198–203 (2010).
[26] P. P. Sahay, S. Tewari, R. K. Nath, S. Jha, and M. Shamsuddin, J. Mater. Sci. **43**, 4534–4540 (2008).
[27] A. Djelloul, M-S. Aida, and J. Bougdira, J. Lumin. **130**, 2113–2117 (2010).
[28] A. Kaushal and D. Kaur, *Effect of substrate temperature on structural, electrical and optical properties of wurtzite and cubic* $Zn_{1-x}Mg_xO$ *thin films grown by ultrasonic spray pyrolysis* (Transport and Optical Properties of Nanomaterials-ICTOPON), eds. M. R. Singh and R. H. Lipson (AIP,2009), p. 339–346.
[29] I. Stambolova *et al.*, Mater. Chem. Phys. **121**, 447–452 (2010).
[30] M. Subramanian, M. Tanemura, T. Hihara, V. Ganesan, and T. Soga, T. Jimbo, Chem. Phys. Lett. **487**, 97–100 (2010).
[31] T. P. Rao and M. C. Santhoshkumar, Appl. Surf. Sci. **255**, 7212–7215 (2009).
[32] K. Ravichandran and P. Philominathan, Sol. Energ. **82**, 1062–1066 (2008).
[33] V. Bilgin, S. Kose, F. Atay, and I. Akyuz, Mater. Chem. Phys. **94**, 103–108 (2005).
[34] P. M. R. Kumar, K. P. Vijayakumar, and C. S. Kartha, J. Mater. Sci. **42**, 2598–2602 (2007).
[35] M. A. M. Khan, M. W. Khan, M. Alhoshan, M. S. AlSalhi, and A. S. Aldwayyan, Appl. Phys. A **100**, 45–51 (2010).
[36] K. Vanheusden *et al.*, J. Appl. Phys. **79(10)** 7983–7990 (1996).
[37] Y. Q. Gao *et al.*, Appl. Phys. A **98**, 129–134 (2010).
[38] C. Ye, S. S. Pan, X. M. Teng, H. T. Fan, and G. H. Li, Appl. Phys. A **90**, 375–378 (2008).
[39] J. M. Bian, X. M. Li, X. D. Gao, W. D. Yu, and L. D. Chen, Appl. Phys. Lett. **84**(4), 541–543 (2004).